A Simple Strip Model in the Volume-Surface Integral Equation for Analysis of Arbitrary Probe-Fed Conformal Microstrip Antennas

Mang He, Qiang Chen, *Member, IEEE*, Qiaowei Yuan, Kunio Sawaya, *Senior Member, IEEE*, and Xiaowen Xu

***Abstract*—A strip model is incorporated in the volume-surface integral equation (VSIE) to simplify the analysis of the probe-fed conformal microstrip antennas (CMSAs) with arbitrary shapes. The thin wire–surface junction of the feeding probe and the patch is transferred to the surface–surface junction that can be modeled by using Rao–Wilton–Glisson (RWG) basis functions easily. Thus, the use of complicated attachment mode basis function in the conventional VSIE is eliminated, which simplifies the calculation of the method-of-moments (MoM) matrix. The construction of RWG basis functions at the surface–surface junction is detailed as well. An effective remedy is also proposed to overcome the computation breakdown in the near-singularity treatment when the field point locates at the extension of one side of the source domain. Numerical results show the reliability and accuracy of the proposed method.**

***Index Terms*—Conformal microstrip antennas (CSMAs), method of moments (MoM), near-singularity, volume-surface integral equation (VSIE).**

I. Introduction

A NUMBER of the method of moments (MoM)-based full-wave solutions have been proposed to analyze the microstrip antennas (MSAs) with various shapes [1]–[4]. Among them, the VSIE method [5] is one of the most attractive approaches due to its flexibility and easy conjunction with the recently developed fast algorithms since only the free-space Green's function is used compared to the surface integral equation (SIE) method [4]. In [3], Lu *et al.* investigated the stripline-fed CMSAs on finite-size substrates by using curvilinear quadrilateral mesh for the metallic surface and hexahedron mesh for the dielectric material in VSIE. However, the probe-feeding structure was not considered. Recently, Yuan *et al.* analyzed the probe-fed CMSAs on finite substrates using the volume-surface-wire integral equation and the pre-corrected-FFT method [4], where the feeding probe, metallic surfaces, and the dielectric volumes were discretized by using the rooftop, RWG [7], and Schaubert–Wilton–Glisson (SWG) [8] basis functions, respectively, while a special attachment mode basis function was employed to simulate the fast varying current at the wire–surface junction [6]. Accurate results can be obtained, but four different types of basis functions were used in that method, which complicated the construction of the MoM matrix and subsequently the implementation of the fast algorithm.

On the other hand, in order to improve the accuracy of the VSIE, the near-singularities should also be dealt with carefully in addition to the self-singularities arising in the MoM matrix, especially when CMSA on thin dielectric substrate is analyzed. This topic has been well documented in the classic paper [9]. However, when the observation point locates at the positive extension of one side of the source triangle or tetrahedron, the formulas in [9] will encounter a numerical breakdown and cannot give the correct result.

In this letter, the aforementioned two issues are addressed. A simple equivalent strip is used to model the feeding probe, transferring the original thin wire-surface junctions of the probe and the radiating patch/ground plane to surface–surface junctions. By properly arranging the RWG basis functions, the current at a junction can be described accurately. This treatment eliminates the use of the attachment mode basis function and thus reduces the computational complexity of MoM matrix since the related basis functions have only two types: RWG basis functions for the metallic surfaces and SWG basis functions for the dielectric volumes. The latter issue is solved by introducing a small deviation from the side extension and using a simple limiting process. Numerical results for the CMSAs with various shapes, compared to the calculated and experimental controls in the published literature, are shown to validate the proposed method.

II. Formulation

A. VSIE and the Strip Model for the Wire–Surface Junction

Fig. 1 shows the geometry of a probe-fed CMSA on an arbitrarily shaped finite substrate. The unknown surface currents on the metallic bodies and the volume currents in the dielectric objects can be obtained by solving the VSIE

$$\frac{\vec{D}(\vec{r})}{\varepsilon(\vec{r})} = \vec{E}^i(\vec{r}) + \vec{E}^s(\vec{r}) \quad \vec{r} \in V \tag{1a}$$

$$\left[\vec{E}^i(\vec{r}) + \vec{E}^s(\vec{r})\right]_{\tan} = 0 \quad \vec{r} \in S \tag{1b}$$

Manuscript received February 09, 2009; revised March 06, 2009. First published March 24, 2009; current version published June 24, 2009. This work was supported in part by the Natural Science Foundation of China under Grants 60801008 and 60871003, the Foundation of the Misnistry of Education of China on Doctoral Programs under Grant 20060007011, and the Global COE program of Tohoku University, Japan.

M. He is with the Department of Electronic Engineering, Beijing Institute of Technology, Beijing, 100081, China, and also with the Department of Electrical and Communication Engineering, Tohoku University, Sendai 980-77, Japan (e-mail: hemang@bit.edu.cn; mang_he@hotmail.com).

Q. Chen, Q. Yuan, and K. Sawaya are with the Department of Electrical and Communication Engineering, Tohoku University, Sendai 980-77, Japan (e-mail: chenq@ecei.tohoku.ac.jp; qwyuan@ecei.tohoku.ac.jp; sawaya@ecei.tohoku.ac.jp).

X. Xu is with the Department of Electronic Engineering, Beijing Institute of Technology, Beijing, 100081, China (e-mail: xuxiaowen_xxw@163.com).

Color versions of one or more of the figures in this letter are available online at http://ieeexplore.ieee.org.

Digital Object Identifier 10.1109/LAWP.2009.2018709

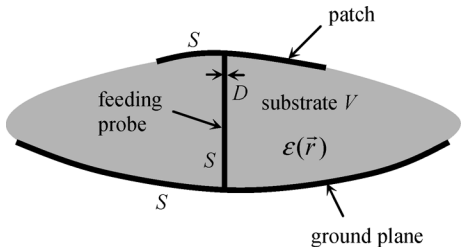

Fig. 1. Cross section of the probe-fed CMSA with arbitrary shape.

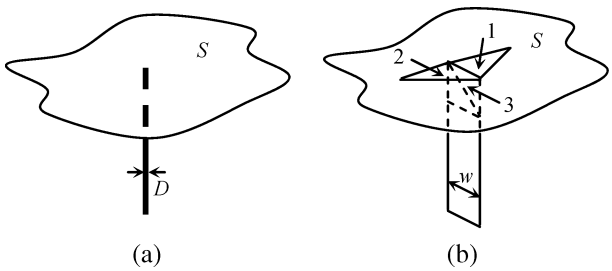

Fig. 2. Wire–surface junction and its equivalent surface–surface junction structure. (a) Wire–surface junction. (b) Surface–surface junction.

where V is the set of the dielectric volumes, and S denotes the surfaces of the metallic bodies. $\vec{D}(\vec{r})$ is the electric flux density in V, while $\vec{E}^i(\vec{r})$ and $\vec{E}^s(\vec{r})$ are the electric field due to the applied source and the scattered field from the induced currents in V and on S, respectively.

The hybrid integral (1) can be solved by using Galerkin's MoM with high accuracy. Using the procedure similar to [4], the dielectric volumes and metallic surfaces are meshed into tetrahedron and triangle cells, and then RWG and SWG basis and test functions are applied to construct the MoM matrix, respectively. However, in this letter, the treatment of the feeding probe and the wire–surface junction is different from [4]. First, the feeding probe of diameter D is replaced by its equivalent strip structure with the width $w = 2D$ [10], and the wire–surface junction is changed to a surface–surface junction, as shown in Fig. 2. Then, the induced electric currents on all of the metallic surfaces can be expanded using RWG basis functions, including the junction part. Therefore, the use of the one-dimensional rooftop basis function for the probe and the attachment mode basis function for the wire-surface junction in [4] is eliminated, which makes the calculation of the matrix element much easier, since the types of the basis functions are reduced from four to two. As seen from Fig. 2(b), there are three triangles, marked as 1, 2, and 3, sharing the surface-surface junction as the common inner side. According to the definition of RWG function [7], three basis functions can be formed; Each is defined on an arbitrary triangle pair combination from these three triangles, i.e. (1,2), (2,3), and (3,1). However, the scattered fields produced by these three basis functions are not independent since these triangles are all in the same medium (free space). Thus, the rows and columns of the MoM matrix related to the junction will be linearly dependent, which makes the matrix singular. The simplest solution is to break the "loop structure" of the basis functions at the junction. That is to say, one of the basis functions should be removed while the choice is arbitrary. This rule also applies

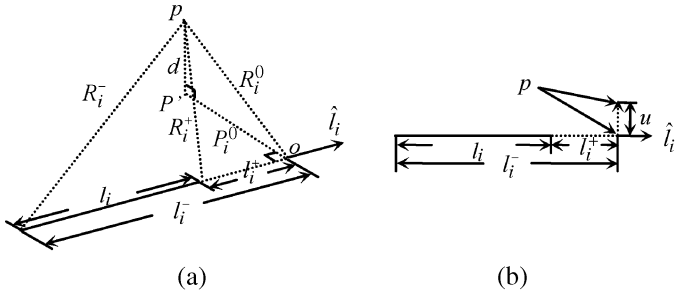

Fig. 3. Definitions of the geometrical parameters in the computation of the singularities and near-singularities. (a) Relative position of the field point to one side of the source domain. (b) Field point resides on the positive extension of one side of the source domain.

to the case where more than three triangles share the common inner side at the junction.

When S denotes the ground plane in Fig. 2(b), the excitation source locates at the junction and can be established by using the delta-gap voltage model

$$\vec{E}^i = \hat{n}_l \delta(l) \tag{2}$$

where $\hat{n}_l$ is normal to the junction and is at the same planes of the positive and negative triangles defined in RWG function, and l is the variable along that direction. It is worth noting that (2) must be enforced on only one of the basis functions at the junction, and this basis function must include a triangle on the equivalent strip of the feeding probe [e.g., triangle 3 in Fig. 2(b)] in order to depict the correct direction of the current flow.

B. A Simple Remedy for the Near-Singularity Computation

In [9], Wilton *et al.* presented comprehensive procedures to evaluate the singular integrals arising in the MoM solution of (1). One common expression in all formulas in [9] is

$$g_i = \ln\left(\frac{R_i^+ + l_i^+}{R_i^- + l_i^-}\right) \tag{3}$$

where $R_i^\pm = \sqrt{l_i^{\pm 2} + P_i^{0 2} + d^2}$ as defined in Fig. 3.

When Dunavant's and Keast's schemes [11], [12] are used for numerical integration in VSIE, the evaluation points are well within the source triangles and tetrahedrons. Therefore, it is very safe to utilize the formations provided in [9] to calculate the singular integrals for self-interactions, in which case the source and field domains are overlapped. However, (3) will pose a numerical problem when the observation point p resides on the positive extension of the side i of the source triangle or tetrahedron. In this situation, (3) becomes

$$\begin{aligned} g_i &= \ln\left(\frac{\left|l_i^+\right| + l_i^+}{\left|l_i^-\right| + l_i^-}\right) \\ &= \ln\left(\frac{\left(\left|l_i^-\right| - l_i\right) + \left(l_i - \left|l_i^-\right|\right)}{\left|l_i^-\right| + l_i^-}\right) = \ln\left(\frac{0}{0}\right) \end{aligned} \tag{4}$$

since $P_i^0 = d = 0$ and $l_i^+, l_i^- < 0$. l_i and $\hat{l}_i$ are the length and the unit positive vector of side i. This is a frequently encountered case in the computation of the near-singularities in VSIE as the

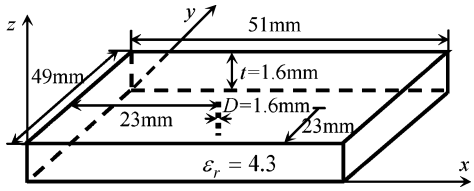

Fig. 4. Geometry of a probe-fed planar MSA.

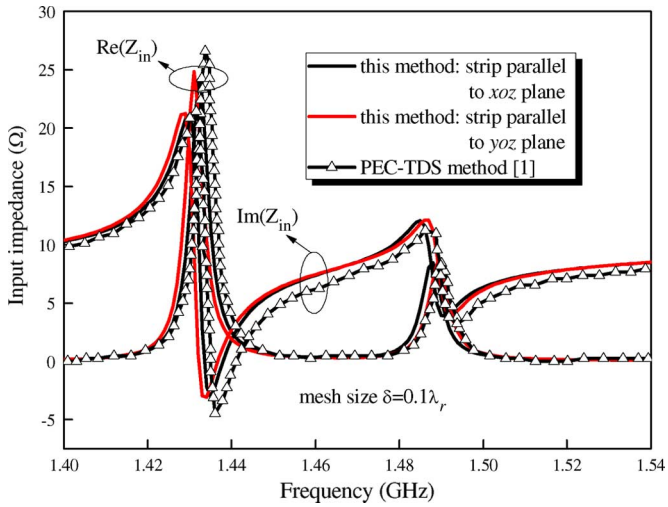

Fig. 5. Input impedance of the planar MSA.

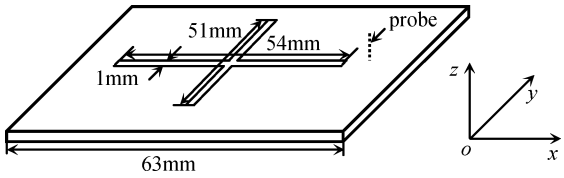

Fig. 6. Geometrical parameters of the cavity-backed cross-slot antenna.

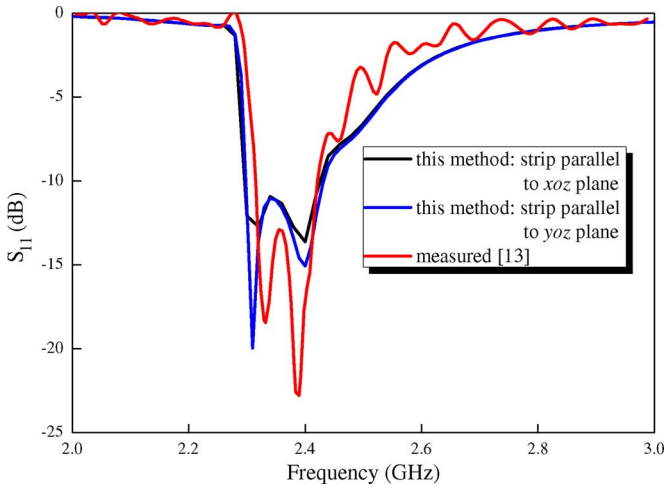

Fig. 7. Simulated and measured reflection coefficient of the antenna.

field point approaches but does not locate within the source domain, especially in the analysis of the CMSA with thin substrate. As a simple remedy to (3), let the field point deviate a small distance u from the extension of the side as in Fig. 3(b), and then take the limit of (4) as u approaches zero

$$g_i = \lim_{u\to 0} \ln\left(\frac{\sqrt{\left(\left|l_i^-\right|-l_i\right)^2+u^2}-\left(\left|l_i^-\right|-l_i\right)}{\sqrt{\left|l_i^-\right|^2+u^2}-\left|l_i^-\right|}\right)$$
$$= \ln\left(\frac{\left|l_i^-\right|}{\left|l_i^-\right|-l_i}\right) = \ln\left(\frac{l_i^-}{l_i^+}\right). \quad (5)$$

Through this modification, the formulas presented in [9] will be more robust when dealing with the near-singularities in the VSIE-based MoM solution.

III. Numerical Results

As the first example, a probe-fed planar MSA is analyzed by using the proposed simplified VSIE method. Fig. 4 shows the geometry of the MSA with the patch, the ground plane, and the finite substrate having the same size in the transverse direction. The input impedance of the antenna is shown in Fig. 5. It is found that good agreement is achieved when our result is compared with that presented in [1]. It is also found that the calculated Z_{in} only varies slightly when the equivalent strip for the feeding probe is parallel to different coordinate planes, which means that the proposed method is not sensitive to the strip orientation around the axis although the strip model does not exhibit symmetry. In the simulation, the average side length δ of the triangles for the patch and ground plane and the tetrahedrons for the substrate is 9 mm, which is about one-tenth of the wavelength at 1.54 GHz in the dielectric. The equivalent strip for the feeding probe is meshed into six triangles. The number of triangle and tetrahedron are 142 and 269, respectively. The total number of unknowns is 833, which is much less than that in [1] where the PEC-TDS, a method based on the reduced surface integral equation, is used. This is due to the fact that in the present model, the feeding probe can be discretized by rather coarse triangle cells, and subsequently the dense tetrahedron meshes in the substrate surrounding the probe and the junction are not needed, which reduces the number of unknowns. The matrix filling and solving time are only 4.0 and 1.2 s, respectively, on a laptop computer with a 2.1-GHz CPU and 2-GB core memory.

Next, a probe-fed, low-profile, cavity-backed cross-slot antenna for satellite radio applications [13] is investigated. The geometrical parameters of the antenna are shown in Fig. 6. The metallic cavity is square in the transverse direction and is filled with a 3-mm-thick dielectric material of $\varepsilon_r = 2.2$, while two slots have the same width and slightly different lengths in order to generate circularly polarized radiation. The feed is offset from the center of the cavity by 23 mm along the diagonal of the cavity. Since the radius of the probe was not specified in [13], it is set to be 0.325 mm in the numerical simulation. In Fig. 7, the computed reflection coefficient of the antenna is compared with the measured one [13], and the good agreement indicates that our model is also accurate for the slot antenna simulation.

Finally, we consider a cylindrically conformal microstrip antenna on a finite substrate. Fig. 8 shows the structure of the antenna. l_g and w_g are the sizes of the substrate, while l and w are the lengths of the patch at the straight and circumferential directions, respectively. The radius of the probe is 0.325 mm, while the feeding point is on the centerline of the curved side and is 10 mm from the center of the patch. The inner radius of curvature of the substrate is $a = 50$ mm. Fig. 9 shows the input impedance of the antenna versus different substrate sizes. It can

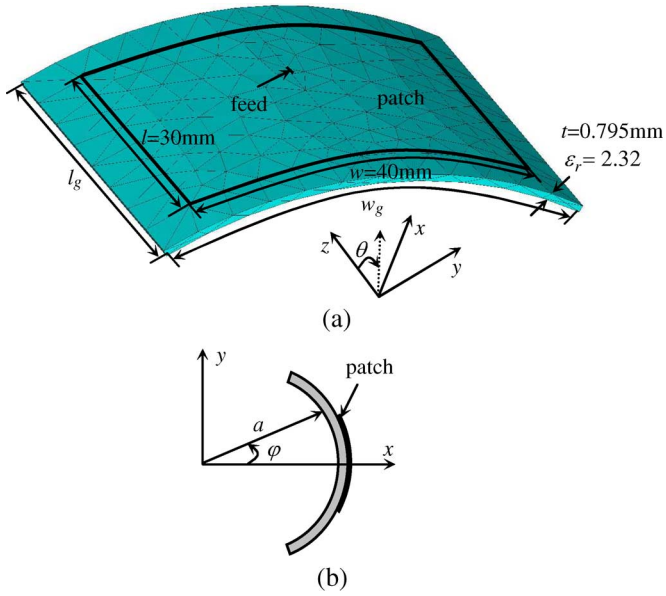

Fig. 8. Geometry of the cylindrical CMSA. (a) 3D view. (b) Side view.

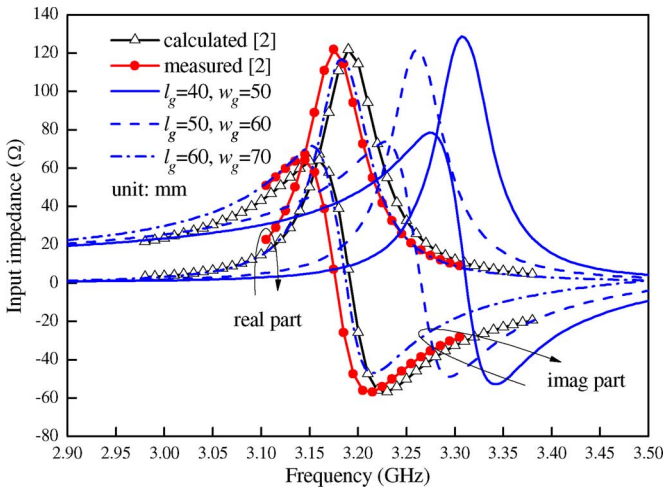

Fig. 9. Input impedance of the antenna with various substrate sizes.

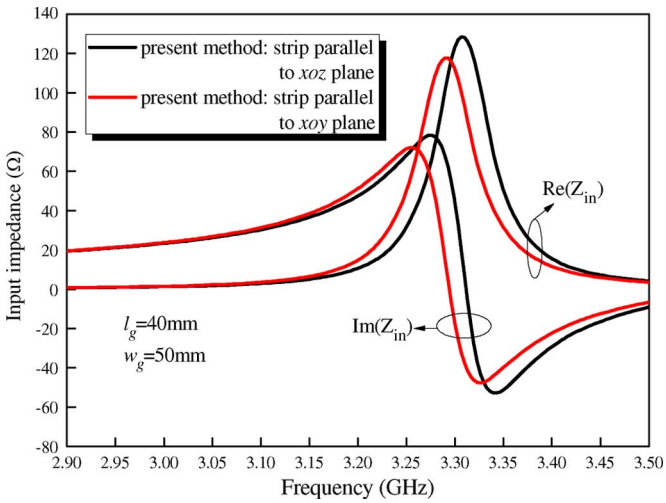

Fig. 10. Input impedance of the antenna with different strip orientation.

be seen that the resonant frequency of the antenna decreases as the substrate size is increased, and the magnitude of the input impedance decreases slightly. When the substrate is enlarged to $l_g \times w_g = 60$ mm $\times$ 70 mm, the input impedance approaches to that of the same patch printed on an infinite long and complete host PEC cylinder of the same radius covered by the same dielectric. Fig. 10 shows the input impedance of the antenna by using different equivalent strip orientation in the probe modeling. It is found that the relative error of the calculated resonant frequencies is less than 1%, and the input impedances also exhibit good agreement.

IV. Conclusion

A simple equivalent strip model is proposed for the analysis of the probe-fed CMSA with arbitrary shape. The wire–surface junction in the conventional VSIE is replaced by a surface–surface junction that can be easily modeled by appropriately arranged RWG basis functions. This modification not only simplifies the construction of the MoM matrix, but also reduces the number of unknowns. Meanwhile, a simple remedy to the classic formula in the previous literature is also presented to make the computation of the near-singularities in VSIE more robust and reliable. Numerical results show the validity and accuracy of the proposed method.

References

[1] I.-T. Chiang and W. C. Chew, "A coupled PEC-TDS surface integral equation approach for electromagnetic scattering and radiation from composite metallic and thin dielectric objects," *IEEE Trans. Antennas Propag.*, vol. 54, no. 11, pp. 3511–3516, Nov. 2006.

[2] M. He and X. Xu, "Closed-form solutions for analysis of cylindrically conformal microstrip antennas with arbitrary radii," *IEEE Trans. Antennas Propag.*, vol. 53, no. 1, pp. 518–525, Jan. 2005.

[3] C.-C. Lu and C. Yu, "Computation of input impedance of printed antennas with finite size and arbitrary shaped dielectric substrate and ground plane," *IEEE Trans. Antennas Propag.*, vol. 52, no. 2, pp. 615–619, Feb. 2004.

[4] N. Yuan, T. S. Yeo, X. C. Nie, Y. B. Gan, and L. W. Li, "Analysis of probe-fed conformal microstrip antennas on finite grounded substrate," *IEEE Trans. Antennas Propag.*, vol. 54, no. 2, pp. 554–562, Feb. 2006.

[5] C. C. Lu and W. C. Chew, "A coupled surface-volume integral equation approach for the calculation of electromagnetic scattering from composite metallic and material targets," *IEEE Trans. Antennas Propag.*, vol. 48, 12, no. 12, pp. 1866–1868, Dec. 2000.

[6] H. Jeuland, B. Uguen, G. Chassay, and E. Grorud, "Numerical and experimental processes for the analysis of a wire antenna mounted on a metallic body," *Microw. Opt. Technol. Lett.*, vol. 15, no. 5, pp. 267–272, 1997.

[7] S. M. Rao, D. R. Wilton, and A. W. Glisson, "Electromagnetic scattering by surfaces of arbitrary shape," *IEEE Trans. Antennas Propag.*, vol. AP-30, no. 3, pp. 409–418, May 1982.

[8] D. H. Schaubert, D. R. Wilton, and A. W. Glisson, "A tetrahedral modeling method for electromagnetic scattering by arbitrarily shaped inhomo-geneous dielectric bodies," *IEEE Trans. Antennas Propag.*, vol. AP-32, no. 1, pp. 77–85, Jan. 1984.

[9] D. R. Wilton, S. M. Rao, A. W. Glisson, D. H. Schaubert, and C. M. Butler, "Potential integrals for uniform and linear source distributions on polygonal and polyhedral domains," *IEEE Trans. Antennas Propag.*, vol. AP-32, no. 3, pp. 276–281, Mar. 1984.

[10] C. A. Balanis, *Antenna Theory: Analysis and Design*, 3rd ed. New York: Wiley, 2005.

[11] D. A. Dunavant, "High degree efficient symmetrical Gaussian quadrature rules for the triangle," *Int. J. Numer. Methods Eng.*, vol. 21, pp. 1129–1148, 1985.

[12] P. Keast, "Moderate-degree tetrahedron quadrature formulas," *Comput. Methods in Appl. Mechan. Eng.*, vol. 55, pp. 339–348, 1986.

[13] D. Sievenpiper, H. P. Hsu, and R. M. Riley, "Low-profile cavity-backed cross-slot antenna with a single-probe feed designed for 2.34 GHz satellite radio applications," *IEEE Trans. Antennas Propag.*, vol. 52, no. 3, pp. 873–879, Mar. 2004.